RESEARCH

Data + pilot biases in modern GNSS signals

O. Montenbruck[1] · P. Steigenberger[1] · J. M. Sleewaegen[2]

Abstract

While traditional GNSS signals are always modulated with navigation data, various modern signals provide a distinct pilot channel without data modulation to support long coherent integration times. Intra-signal biases between the data and pilot components of such signals are evaluated for satellites of the GPS, Galileo, BeiDou-3, and QZSS constellations using measurements from a dedicated set of receivers. Peak values of about 2 ns are obtained for the GPS L5 signal, while slightly smaller values of up to 1 ns apply for the B1C and B2a signals of BeiDou-3 as well as the QZSS L1C signal. For Galileo E1 and E5a/b, data + pilot biases are confined to less than 0.1–0.3 ns, which is typically less than other pseudorange errors for these signals. Fully negligible values of < 0.05 ns are obtained for the L1C and L2C signals of GPS as well as the L2C signal of QZSS in accord with expectations for time-multiplexed or interlaced modulations. To support consistent processing of multi-GNSS data in heterogeneous networks, biases between combined data + pilot tracking and pilot-only tracking are derived in a dedicated zero-baseline receiver test bed. The analysis confirms the general understanding that biases between combined and pilot-only pseudoranges amount to a fixed fraction of the corresponding data + pilot biases. This fraction depends on the power sharing of the data and pilot component in the respective signals and amounts to 50% in most cases. The results of this study are expected to remove the prevailing problem of two distinct receiver groups in the generation of satellite clock and bias products by the International GNSS Service and to enable a rigorous and consistent use of these products by multi-GNSS users.

Keywords Biases · Data channel · Pilot channel combined tracking

Introduction

A variety of modernized navigation signals of GPS/QZSS (L1C, L2C, L5), Galileo (E1 Open Service, E5a, E5b), and BeiDou-3 (B1C, B2a) presently offer distinct channels with and without modulated navigation data (Betz 2016). Depending on the specific signals and constellations, the data and pilot channels are modulated on the common carrier using different modulation techniques, including time multiplexing, phase quadrature, or interplex modulation, and make use of distinct pseudo random noise (PRN) ranging codes. While the data channel always needs to be demodulated to access the corresponding navigation data, the actual tracking can be confined to the data-less pilot signal, which does not exhibit unknown bit transitions and enables particularly long coherent integration times. Therefore, geodetic receivers commonly track the pilot component for the generation of high-grade pseudorange, carrier phase, and Doppler measurements while using only a slaved prompt correlator arm on the data channel for demodulating the data bits of such signals. Alternatively, a combined tracking loop making joint use of correlation samples from the pilot and data channels is employed in various receiver architectures to benefit from the combined signal power and to achieve a higher carrier-to-noise density ratio (C/N_0).

In the combined ("x") tracking mode, independent correlation or discriminator values are obtained for each of the two signal components and used to form a combined measurement of the tracking error for the code- and phase-tracking loops. In this way, a lower tracking noise is achieved,

✉ O. Montenbruck
oliver.montenbruck@dlr.de

P. Steigenberger
peter.steigenberger@dlr.de

J. M. Sleewaegen
jm.sleewaegen@septentrio.com

[1] German Space Operations Center, Deutsches Zentrum für Luft- und Raumfahrt (DLR), 82234 Weßling, Germany

[2] Septentrio, 3001 Leuven, Belgium

which corresponds to the C/N$_0$ for the total signal power received for the two channels.

In the presence of biases between the data ("d") and pilot ("p") components, the combination will result in a distortion of the combined correlation functions and a shift of the tracking point. The shift will depend on the combining method. In the case where the combination involves adding the pilot and data correlations prior to computing the discriminator, it can be modeled in analogy with short range multipath (Byun et al. 2002; Young and Meehan 1988) for in-phase signals. For a typical early-minus-late correlator and for a given data-minus-pilot bias B_{d-p}, the combined tracking will then result in the bias

$$B_{x-p} = B_{d-p} \cdot \frac{\alpha}{1+\alpha} \tag{1}$$

with respect to the pilot-only tracking, where α denotes the amplitude ratio of the data component relative to the pilot component.

In view of the small magnitude of data + pilot biases for current GNSS signals in relation to commonly employed correlator spacings, Eq. (1) is likewise applicable for more advanced correlator architectures such as double-delta and strobe correlators and can be used as a baseline for modeling the expected biases of combined data + pilot tracking relative to the pilot-only tracking. Nevertheless, it must be emphasized that implementation details for the combined tracking mode are not disclosed by the current receiver manufacturers. As such, the above model represents a conceptual model, but cannot necessarily substitute actual measurements of x–p biases. In particular, this applies to signals with different power in the data and pilot channel, such as QZSS L1C and BeiDou B1C, where non-identical weights may be applied in combination to minimize the resulting code tracking noise (Hegarty 1999; Guo et al. 2022).

To distinguish the various modes of tracking and measurement generation, the Receiver INdependent EXchange (RINEX, Romero 2021) format provides distinct observation codes such as D (data) and P (pilot), I (in-phase) and Q (quadrature), S (short) and L (long), or B and C for data-only and pilot-only tracking. In contrast, the X and, occasionally, Z observation codes are used for measurements resulting from the combined tracking of the two signal components. The proper assignment and careful distinction of observation codes is a necessary condition for considering tracking-mode-specific signal biases in the processing of GNSS observations, but has not been applied and exploited in an adequate manner, so far.

Within the global monitoring network of the International GNSS Service (IGS, Johnston et al. 2017), a heterogeneous set of receivers is used for tracking satellites of the various global and regional satellite navigation systems. Measurements of the IGS network provide the basis for the determination of precise orbit and clock products, which in turn support a multitude of GNSS applications in the field of surveying, timing, and geodesy. Since the various receiver models available within the IGS provide either x- or p-tracking observations but do not offer concurrent measurements from both modes, the IGS network essentially partitions into two distinct groups of stations (Wang et al. 2016). This division causes both conceptual and practical problems in the joint processing of data from the x and p receiver groups in the orbit determination and time synchronization (ODTS) of GNSS satellites (Montenbruck and Steigenberger 2021) and the use of the resulting products in precise point positioning (PPP; Li et al. 2020).

Even though carrier phase observations from both receiver groups can provide precise information on the variation of satellite clock offsets over time, rigorous use of pseudorange measurements from both receiver groups for absolute clock offset determination is hampered by the presence of satellite-specific x–p biases, whenever the conventional clock reference signals involve both pilot and data components. Here, satellite clock offsets must either be referred to pilot-only tracking or combined data + pilot tracking and only pseudoranges from the corresponding group of receivers should be used in the ODTS process. While GPS is not currently affected by this issue due to the use of the L1/L2 P(Y) signals as the basic clock reference, the ionosphere-free E1/E5a combination is commonly used as a reference for the precise orbit and clock products of Galileo within the IGS. This leaves an ambiguity concerning the choice of pilot or combined data + pilot observations on both frequencies, which analysis centers and users often silently ignore. Signals with data and pilot components also serve as the clock reference for QZSS (L2C) and are likely to be applied for BeiDou-3 (B1C, B2a) in the foreseeable future.

With this background, the present study aims to comprehensively characterize biases in open-service data/pilot signals of the various global and regional navigation satellite systems based on actual receiver measurements. In addition, first calibrations of x–p satellite biases for the relevant signals of GPS, Galileo, and BeiDou-3 are provided that will assist consistent processing of combined data + pilot and pilot-only observations from the respective receiver groups in a heterogeneous tracking network.

Data and processing

The results discussed in this work are based on measurements collected with two basic receiver types specifically configured or modified to support independent and concurrent tracking of data and pilot channels. Following the initial work of Sleewaegen and Clemente (2018), a new and comprehensive set of data + pilot biases for four constellations was determined for the present study with two Septentrio

PolaRx5 receivers in Leuven and Tokyo in January 2023. Other than the standard firmware, limited to pilot-only measurements, a special firmware build was used in both campaigns to support joint tracking and output of data and pilot observations. Overall, data + pilot biases for the GPS L1C, L2C, L5, Galileo E1 O/S, E5a, E5b, and BeiDou-3 B1C, B2a signals were obtained for the globally visible satellites in medium earth orbit. In addition, L1C, L2C, and L5 biases were measured for the QZSS satellites in both inclined geosynchronous and geostationary orbit.

Next to the PolaRx5, measurements of GPS, Galileo, and BeiDou-3 data + pilot biases for the aforementioned signals were performed at DLR's German Space Operations Center (GSOC), Oberpfaffenhofen, in January 2023 with a pair of Javad TRE-3S receivers in zero-baseline configuration. While one of the two receivers was operated in the default configuration for combined data + pilot tracking with "normal" correlator settings, the second receiver was operated in a special "data" configuration providing distinct data and pilot observations. RINEX observation files for the two receivers were generated from binary receiver data in the vendor-specific JPS format (Javad 2022) using a conversion software (JPS2Rnx) independently developed by the authors.

Given the limited QZSS visibility from Central Europe, complementary QZSS observations were obtained with Javad TRE-3 receivers of the Multi-GNSS Integrated Real-time and Archived Information system (MIRAI; Cabinet Office 2022a) between January and December 2022. A total of eight stations in the Asia-Pacific region contributed by the QZS operator and supporting joint output of data and pilot observations for GPS and QZSS satellites was selected for this purpose. RINEX observation files for the MIRAI stations are generated by the MIRAI providers based on real-time data streams with multi-signal messages (MSM) in Radio Technical Commission for Maritime Services (RTCM) v3.3 format (RTCM 2021). Due to apparent encoding errors, the designations for data and pilot observations are swapped in both the RTCM real-time streams and the RINEX observation files. For proper data analysis, the respective measurements were therefore exchanged prior to using them in the present analysis.

For comparison with estimated data + pilot code biases, "inter-signal corrections" (ISCs) are used, which are transmitted within the navigation messages of most of the modernized signals. The respective values were extracted from RINEX 4 navigation data files (Montenbruck and Steigenberger 2022) provided by the IGS and represent average values over the January to December 2022 time frame.

The estimation of intra-signal biases B_{d-p} from pseudorange observations P_d and P_p of the data and pilot channels obtained within a single receiver follows the general concept of differential code biases (DCBs) determination of Montenbruck et al. (2014). However, no global ionosphere maps are required for correcting differential path delays between data and pilot signals in view of the common signal frequency. Accordingly, the difference between the data and pilot pseudoranges may be modeled as the sum of the corresponding receiver and satellite biases as well as the receiver noise difference ε_{d-p}:

$$P_d - P_p = B_{d-p}^{rcv} + B_{d-p}^{sat} + \varepsilon_{d-p} \qquad (2)$$

The sum of the receiver and satellite biases is thus obtained as the arithmetic average of the respective data-minus-pilot pseudoranges over the selected data arc. For the separation of satellite and receiver biases, a zero-mean constraint is applied over the satellites of each constellation.

As an alternative to the above approach, inter-signal biases for two signals s_A and s_B of the same frequency or two different tracking modes of the same signal may also be determined using a pair of receivers A and B in zero-baseline configuration, i.e., connected to the same antenna via a power splitter (Hauschild and Montenbruck 2016). In this case, the model for the respective pseudorange difference is given by

$$P_{B,s_B} - P_{A,s_A} = \left[c \cdot dt_{B-A} + B_{B,s_B-A,s_A}^{rcv} \right] + B_{s_B-s_A}^{sat} + \varepsilon_{B-A} \quad (3)$$

where $c \cdot dt_{B-A}$ denotes the product of the speed of light and the differential receiver clock offset at the measurement epoch. Assuming constancy of the satellite biases over the processing interval, the epoch-wise values of the combined clock offset and receiver bias terms as well as the individual satellite biases can be obtained from the solution of a least-squares system based on observations covering an extended data arc and the full constellation. Similar to the single-receiver case, the system exhibits a rank − 1 deficiency that is removed by an additional zero-mean constraint across all observed satellites of the constellation.

Due to the estimation of epoch-wise parameters, the least-squares adjustment involves a substantially larger number of solve-for parameters than the single-receiver, bias-only problem. In view of the block diagonal structure of the normal equations and the purely diagonal structure of the large submatrix for the epoch parameters, the system can, nevertheless, be solved with moderate computational effort, even for long data arcs. Within the present study, a dual-receiver, zero-baseline configuration is used to determine biases between observations for combined data + pilot tracking mode and pilot-only mode, which cannot be generated simultaneously by a single receiver.

Results

Based on the concepts and data sets introduced above, data + pilot biases as well as biases of combined data + pilot tracking with respect to pilot-only tracking have been obtained. Results for the two types of biases in GPS, Galileo, BeiDou-3, and QZSS signals are presented and discussed in this section.

Data + pilot biases

For the L1C and L2C signals of GPS, the satellite-specific data + pilot biases as measured in the present analysis are confined to magnitudes of less than about 0.05 ns (1.5 cm), which is generally negligible in practical GNSS data analysis (Fig. 1). Based on tests for different days, arc lengths and elevation cutoff angles, the individual bias estimates exhibit an uncertainty of about 0.02 ns, close to the magnitude of the bias values themselves. The near-absence of data + pilot biases is indeed expected for the time-multiplexed

modulation of the data (medium length) code and the data-less (long) pilot code in the L2C signal. Similar considerations hold for the data and pilot components of the L1C signal, which is transmitted by the GPS III satellites along with the P(Y) signal in the in-phase channel of the L1 carrier using an interlaced majority voting combination (Spilker and Orr 1998, Thoelert et al. 2019).

On the other hand, pseudorange differences for GPS L5 pilot and data tracking cover a range of about ± 3 ns or, equivalently, ± 90 cm (Fig. 1). This is well above the noise and multipath level of the respective observations and clearly needs to be considered in high precision processing. Within the GPS constellation, L5 data + pilot biases of the GPS III satellites clearly show a notably smaller magnitude and scatter than those of the previous generation of Block IIF satellites. This improved performance is likely related to the use of a mostly digital signal generation chain in GPS III (Marquis and Shaw 2011), which allows for more uniform chip shapes across the individual satellites of the constellation than the earlier analog Block IIF signal generators.

Comparison of the PolaRx5 and TRE-3S results shows agreement at the level of 0.05 ns, and the consistency with
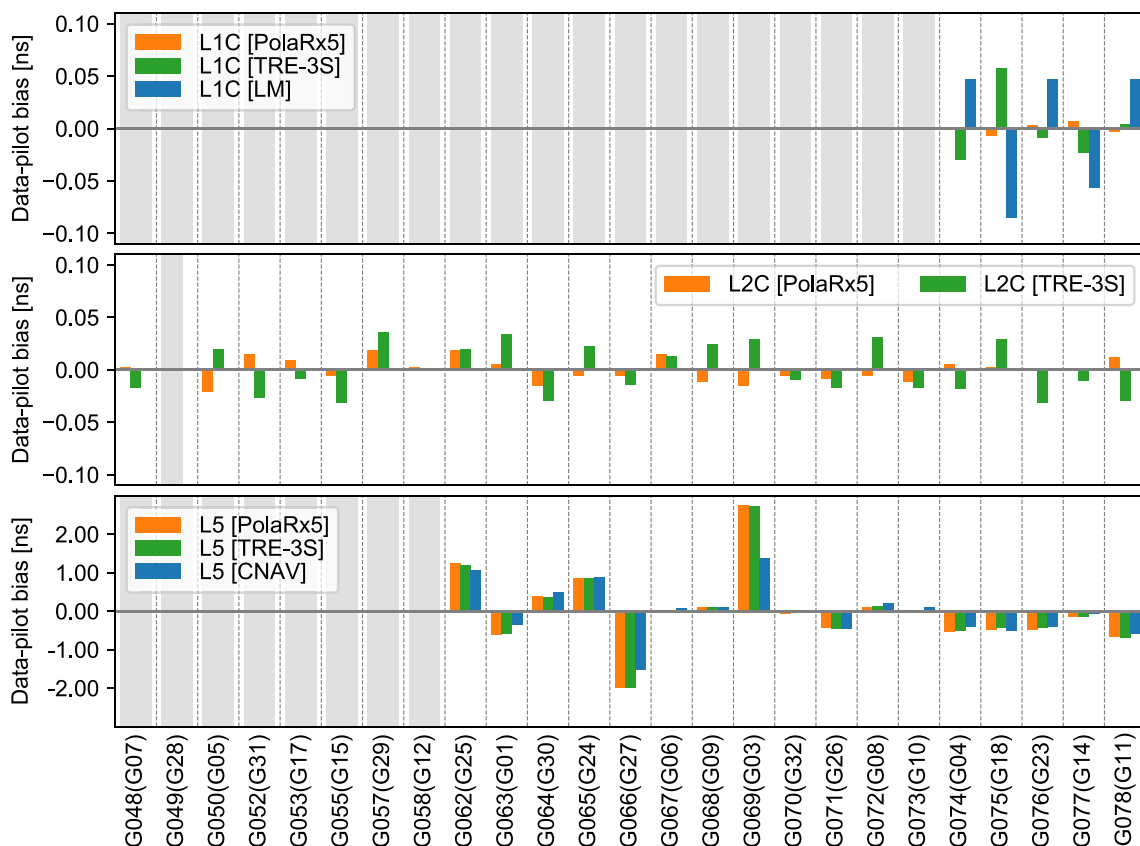

Fig. 1 Data + pilot code biases of modernized GPS signals as obtained with two different receiver types. For L1C and L5, the receiver measurements are compared against zero-mean aligned ISCs

from manufacturer calibrations of Lockheed Martin (LM) and the CNAV navigation message. Shaded bars indicate that the respective biases are not available or not applicable for the given satellite
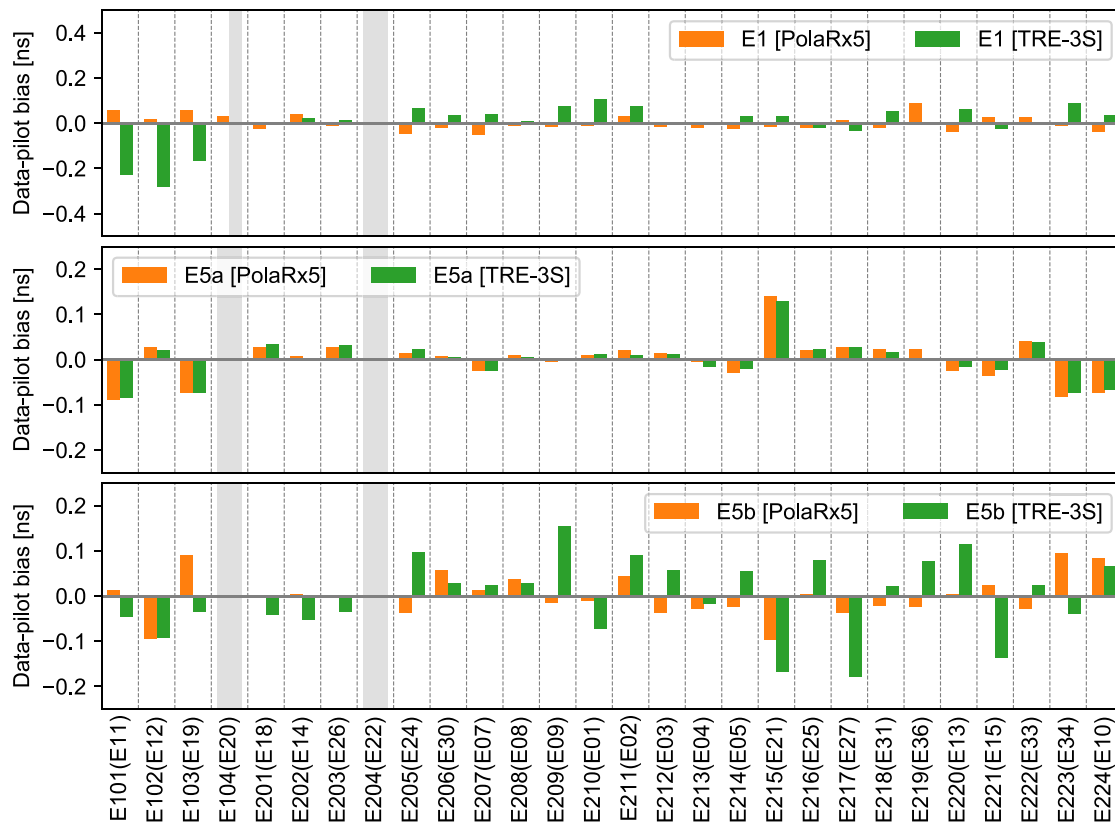
Fig. 2 Data + pilot code biases of Galileo signals as obtained with two different receiver types. Shaded bars indicate that the respective biases are not available or not applicable to the given satellite

zero-mean aligned L5 broadcast ISCs is typically at the 0.1–0.2 ns level. As an obvious exception, a discrepancy of 1.3 ns between receiver measurements and ISCs may be observed for space vehicle number (SVN) G069. While ISCs for L1C are foreseen as part of the new CNAV-2 navigation message, routine transmissions of such messages on the L1C signal will only commence after the introduction of the new OCX control segment for GPS. Initial ISCs for the first five GPS III satellites have, however, been released by the United States Coast Guard Navigation Center (USCG 2022) based on factory calibrations of Lockheed Martin. The respective values suffer from an obvious discretization of the group delay measurements but confirm that the L1C ISCs of all GPS III satellites launched until 2022 are well below the 0.1 ns level after a zero-mean alignment and, therefore, negligible in practical applications.

Galileo data + pilot biases for the E1 Open Service (O/S) signal as well as E5a and E5b amount to typically 0.1 to 0.3 ns, or, equivalently, 3–9 cm (Fig. 2). As already pointed out by Gunawardena et al. (2015), Galileo clearly benefits from the use of a digital frequency generation and up-conversion unit (FGUU) that minimizes chip shape distortions and chip shape variations across different satellites. This

results in a lower scatter of satellite-specific biases in general and better consistency of pilot and data channel group delays. At the given magnitude, data + pilot biases of the Galileo signals are likely buried in measurement noise and multipath for most receivers. Nevertheless, proper consideration of these biases appears advisable when aiming at applications requiring the highest accuracy in the pseudorange modeling for, e.g., timing applications and the generation of high-end orbit and clock products.

For E5a, good consistency of results from both receiver types is obtained, whereas the E1 data + pilot biases exhibit obvious differences in magnitude and even signs. The inconsistencies are most pronounced for the In-Orbit-Validation (IOV) satellites (E101–E103), even though the measured biases are still confined to the 0.2 ns level for all satellites. The receiver dependence suggests a notable impact of the specific correlator architecture and might be more pronounced for E1 than E5a due to the specific properties of the sub-carrier modulation of the Galileo E1 O/S signal. For E5b, major differences between results from the two receiver types are likewise noted. This is surprising, though, in view of the good consistency observed for E5a and the overall similarity of those two signals.
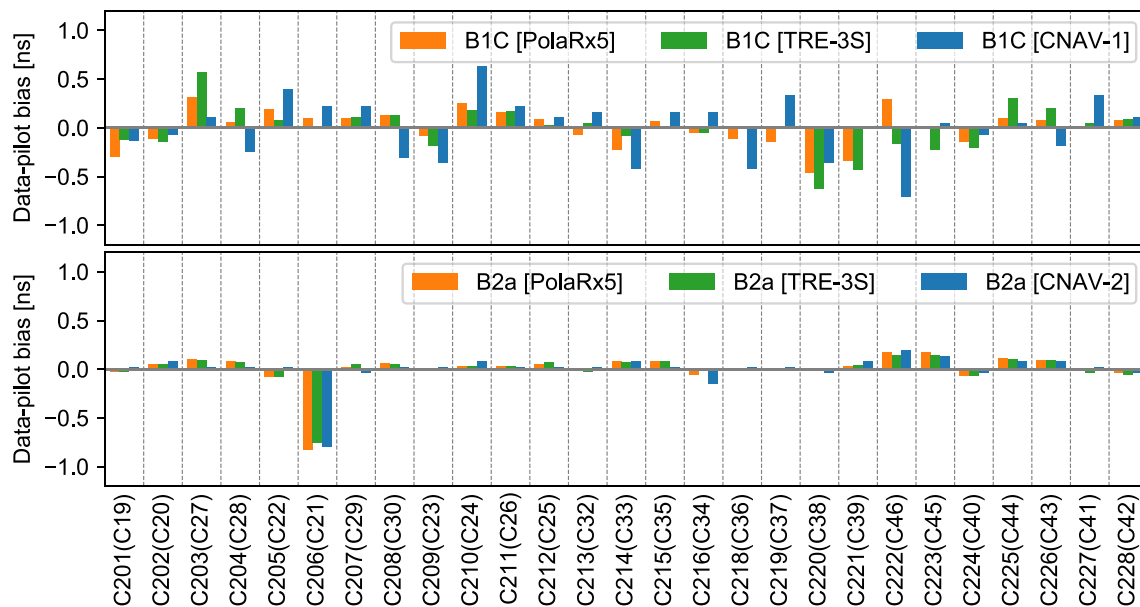
Fig. 3 Data + pilot code biases of BeiDou-3 signals as obtained with two different receiver types. For comparison, zero-mean aligned inter-signal corrections transmitted in the CNAV-1 and CNAV-2 navigation messages are shown

For the new B1C signal of BeiDou-3, data + pilot code biases amount to up to 0.6 ns (Fig. 3), which clearly exceeds the corresponding values for the GPS L1C and Galileo E1 O/S signals in the same frequency band. Differences between the two receiver types can amount to a few tenth of ns for selected satellites, which likely relates to receiver-specific implementations for tracking the quadrature multiplexed binary offset carrier (QMBOC, Lu et al. 2019) modulation. Furthermore, obvious discrepancies between receiver measurements and ISCs, as reported in the CNAV-1 message of the B1C signal, are encountered. In the case of the B2a signal, only small (< 0.15 ns) data + pilot biases are observed for all satellites except for SVN C206, which exhibits a non-negligible bias of about 0.75 ns. Similar to the Galileo E5a signal, good consistency between the estimates from different receiver types is obtained for B2a. Likewise, the present estimates show good agreement with the B2a data + pilot group delays, i.e. the B2ad ISCs, from the CNAV-2 navigation message. It may be noted that the broadcast ISC_{B2ad} values exhibit a mean value of about −2.7 ns across the constellation that notably exceeds the scatter across the various satellites and presently lacks a proper explanation (Montenbruck et al. 2022). As for the signals discussed before, the constellation mean has therefore been removed from the ISCs for the comparison with observed data + pilot biases in Fig. 3.

For QZSS, PolaRx5 receiver measurements of J002–J005 conducted for the current study in January 2023 have been merged with earlier results of Sleewaegen and

Clemente (2018) for J001, while the TRE-3 results are based on MIRAI data for the January to December 2022 timeframe and include both the first QZS-1 satellite (J001; transmitting until March 2022) and the QZS-1R replenishment satellite (J005).

Overall, data + pilot biases of 0.5 to 1 ns are observed for both the L1C and L5 signal (Fig. 4). For L2C, negligible data + pilot biases are encountered, as can be expected for the time-multiplexed modulation. Other than GPS, which uses an interlaced majority voting for the in-phase L1 signal components, the L1C data and pilot components of QZSS are generated using an interplex modulation (Kogure et al 2017). As such, QZSS L1C data + pilot biases in QZSS are generally larger than those of GPS and also larger than those of the time-multiplexed L2C signal. They also exceed those of the Galileo E1 O/S signal, which makes use of a similar interplex modulation. While the L1C data + pilot bias for the Block I QZSS satellite J001 has a magnitude of roughly 0.5 ns, values for the subsequent Block II and IIA satellites are typically at the 0.1–0.2 ns level. L5 data + pilot biases, in contrast, are confined to roughly 0.2 ns across all generations of satellites.

As a peculiarity, we also note the occurrence of orbit-periodic variations with a peak-to-peak amplitude of up to 0.3 ns in the time series of L5 data + pilot pseudorange differences for the Block II and IIA satellites that stand out clearly above the measurement noise. The data + pilot bias variations across an orbit show a distinct pattern that
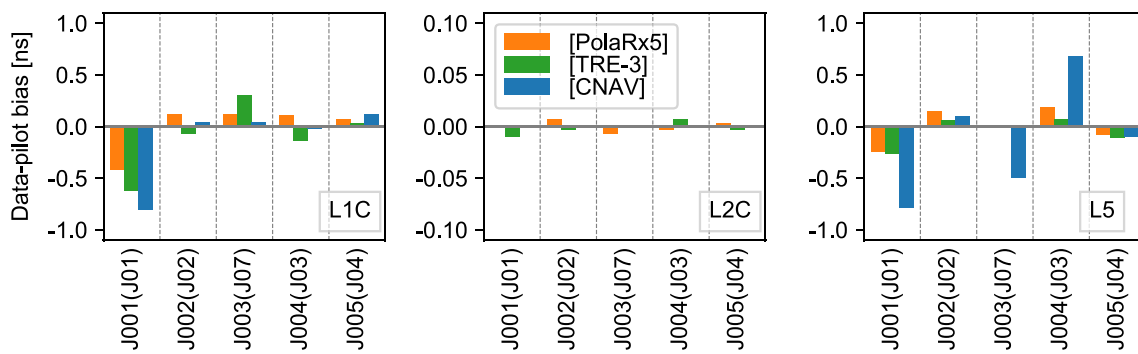
Fig. 4 Estimated data + pilot code biases of QZSS signals as obtained with two different receiver types. For the PolaRx5 receiver, measurements of J002–J005 have been complemented with J001 data of Sleewaegen and Clemente (2018) after adjusting an offset in the biases for the commonly observed J002–J004 in both date sets. For comparison, inter-signal corrections transmitted in the CNAV and CNAV-2 navigation messages are shown

differs with the geographic location of the observing stations. This hints at satellite-generated interference, but further investigations will be required to understand the nature of these variations fully. For the present analysis, Fig. 4 provides mean values of the data + pilot biases over the full visibility period and, in case of the TRE-3 results, over a geographically diverse set of stations.

Differences between data + pilot estimates from the two types of receivers amount to 0.25 ns and 0.1 ns for L1C and L5, respectively. However, major inconsistencies of 0.5–1 ns can be observed in comparison with the long-term mean values of the L5 broadcast ISCs from the CNAV-1 message over the analysis period. The CNAV-1 L5 ISCs are also found to exhibit notable long-term variations with peak-to-peak amplitudes of up to 0.7 ns for the geostationary QZS-3 satellite (J003) that presently lack proper understanding and explanation. No such variations are encountered for the L1C ISCs transmitted in the CNAV-2 message of QZSS, which also show a better overall match with the observed data + pilot biases. Overall, the results hint at a possible deficiency in the ISC calibration of the QZSS ground segment rather than pronounced variability of the actual satellite biases.

Biases of combined data and pilot tracking

While the above measurements provide insight into the magnitude of data + pilot biases in the various GNSS signals, knowledge of these biases themselves is of only limited practical relevance for the processing of multi-GNSS observations from heterogeneous receiver networks due to the sparse availability of geodetic receivers providing measurements from data-only ("d") tracking. Instead, the combined data-plus-pilot ("x") tracking is most widely used as an alternative to pilot-only ("p") tracking and requires a distinction of

the respective receiver groups in the determination of signal biases, clock offsets, and ionosphere products.

Complementary test data for the estimation of x–p biases were collected in a dedicated receiver test bed to cope with this limitation. In the absence of GNSS receivers offering concurrent measurements from all three tracking modes, a pair of TRE-3S receivers in zero-baseline (ZB) configuration was used for our analysis. While one of the receivers was configured for combined data + pilot tracking, the second receiver provided individual pilot-only and data-only observations. Satellite-specific biases were then adjusted from the between-receiver single-difference observations along with epoch-wise single-difference clock offsets.

Scatter plots of the resulting combined-minus-pilot-only biases versus the data-minus-pilot biases are shown in Fig. 5. It covers all GPS, Galileo, and BeiDou-3 signals with relevant intra-signal biases, whereas signals based on time multiplexing and interlaced majority voting have been excluded in view of their negligible data + pilot biases.

With the exception of the BDS B1C signal, all considered signals employ a 1:1 share of signal amplitudes and powers in the data and pilot channels. In accordance with expectations, the respective scatter plots show that the magnitude of x–p biases is close to 50% of the corresponding d–p biases. For the BDS B1C signal, the data and pilot channels are transmitted with a 1:3 power ratio (CSNO 2017), which corresponds to an amplitude ratio of $\alpha = 1/\sqrt{3} \sim 0.58$. Using the model of (1), x–p biases are expected to amount to 37% of the d–p biases in this case, which is in fair agreement with the measured value of 29% but may also relate to different weights in the combination of discriminator values for the combined data + pilot tracking in the tested receiver.

For QZSS, no direct measurements could be performed due to lacking visibility of QZSS satellites at the location
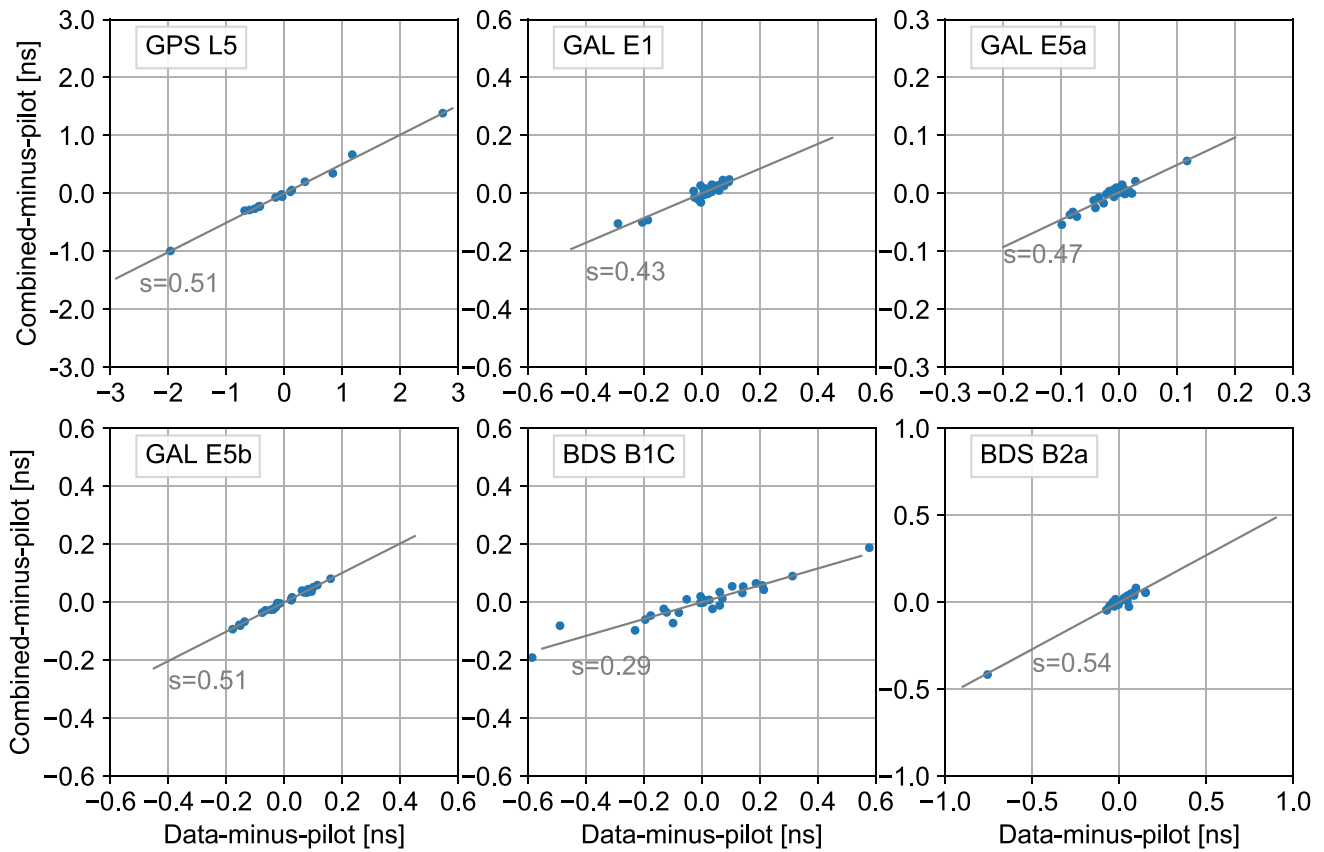
Fig. 5 Scatter plot of TRE-3S x–p biases versus d–p biases for GPS, Galileo, and BeiDou signals with non-negligible data+pilot biases. Next to the individual data points, a regression line and the respective slope are provided

of our zero-baseline test facility. Based on the common signal structure and properties of QZSS L5 and GPS L5, it is reasonable to expect x–p biases of half the size of d–p biases for QZSS L5 as well. For QZSS L1C, in contrast, the data-to-pilot power ratio amounts to 4.8 dB or, equivalently, 1:3 (Cabinet Office 2022b), rather than the common ratio of 1:1. Similar to the BeiDou-3 B1C signal, the x–p biases of QZSS L1C are therefore expected to amount to roughly one-third of the d–p biases in this case.

In the absence of a zero-baseline test bed in the Asia–Pacific regions that could be used for direct estimation of QZSS x–p biases, we indirectly determined L1C x–p biases by differencing the L1C(x)–L1C/A and L1C(p)–L1C/A biases of two independent sets of TRE-3 receivers from the IGS and MIRAI networks, respectively. Using data for J001–J005 from the January to December 2022 time frame, a value of 0.28 for the ratio of x–p biased relative to d–p biases was determined from QZSS L1C signal, which closely matches the B1C value obtained above.

Overall, the results show that the "multipath" model (see (1)) provides a reasonable approximation for the satellite-specific biases of combined tracking relative to pilot-only tracking for the analyzed signals in the present

tests. It should be emphasized, though, that the results are limited to a single-receiver type and correlator architecture for the p-, d-, and x-tracking modes. Further measurements with other receiver types and signals are encouraged to better understand combined tracking modes across diverse hardware platforms and fully characterize the associated biases.

Discussion

As derived in the previous section, the availability of measured x–p satellite biases provides the basis for a proper formulation of the GNSS pseudorange model and enables consistent use of receivers with x- and p-tracking for ODTS and PPP. Considering a single-constellation model and focusing on the relevant contributions, pseudoranges for pilot-only and combined tracking can be described as

$$
\begin{aligned}
P_{\mathrm{p}} &= \rho + c \cdot \left(dt_{\mathrm{p}}^{\mathrm{rcv}} - dt_{\mathrm{ref}}^{\mathrm{sat}} \right) + T + I + B_{\mathrm{p-ref}}^{\mathrm{sat}} \text{ and} \\
P_{\mathrm{x}} &= \rho + c \cdot \left(dt_{\mathrm{x}}^{\mathrm{rcv}} - dt_{\mathrm{ref}}^{\mathrm{sat}} \right) + T + I + B_{\mathrm{p-ref}}^{\mathrm{sat}} + B_{\mathrm{x-p}}^{\mathrm{sat}},
\end{aligned}
\tag{4}
$$

respectively. Here, ρ denotes the light-time corrected geometric range, T and I are the tropospheric and ionospheric range delays; satellite and receiver clock offsets are described by dt^{sat} and dt^{rcv}, $B_{\text{p-ref}}^{\text{sat}}$ is the satellite's differential code bias between the pilot signal and the clock reference signal, and $B_{\text{x-p}}^{\text{sat}}$ is the satellite-specific bias of combined versus pilot-only tracking.

Receiver biases are not explicitly considered in (4) but are lumped into the signal-specific receiver clock offsets. This is adequate based on the understanding that a single receiver will only ever provide either x or p observations, so only one of the two variants of the pseudorange model will be applied for the processing of measurements from a given station. Since no need arises to align clock offsets from different receivers to a common tracking mode in common ODTS or PPP applications, receiver biases can readily be lumped with the receiver clock offset and estimated as a combined parameter.

For satellite biases, in contrast, we distinguish between the bias $B_{\text{p-ref}}^{\text{sat}}$ of pilot-only observations relative to the clock reference signal (ref) and the corresponding bias

$$B_{\text{p-ref}}^{\text{sat}} + B_{\text{x-p}}^{\text{sat}} = B_{\text{x-ref}}^{\text{sat}} \tag{5}$$

for combined tracking, which is split into the sum of the pilot-only bias $B_{\text{p-ref}}^{\text{sat}}$ and the intra-signal x–p bias $B_{\text{x-p}}^{\text{sat}}$. While the first term can be computed from signal-specific satellite biases that are routinely determined by various IGS analysis centers (Wang et al. 2016; Montenbruck et al. 2014; Villiger et al. 2019) and made available for ODTS and PPP users, the $B_{\text{x-p}}^{\text{sat}}$ contribution has commonly been neglected so far.

This simplification has mainly affected the processing of observations from the Galileo constellation, for which the E1 O/S and E5a signals have been adopted as clock reference signals of the precise orbit and clock products. As discussed above, both data-minus-pilot and combined-minus-pilot biases of the Galileo signals are sufficiently small to tolerate the resulting errors, even though further quality improvements can be expected from a proper modeling of p and x observations in accord with (4). Similar considerations hold for QZSS, where data and pilot components of the L2C signal are generated in a time-multiplexed modulation with essentially vanishing relative delays. As such, it is likewise safe to neglect the $B_{\text{x-p}}^{\text{sat}}$ contribution when working with the QZSS L2C signal. The same would not apply, though, when processing L1C instead of the more common L1 C/A code signal. In view of the more pronounced data + pilot biases of QZSS L1C as compared to L2C, proper consideration of $B_{\text{x-p}}^{\text{sat}}$ would obviously be needed in this case.

Likewise, $B_{\text{x-p}}^{\text{sat}}$ will need to be considered when working with the modernized B1C and B2a signals in the processing of BeiDou-3 observations. The two signals are particularly attractive due to their common frequencies with GPS L1/L5 and Galileo E1/E5a as well as improved signal properties (Montenbruck et al. 2020) and have already shown a superior performance in ODTS and PPP compared to the legacy B1I/B3I signals (Wang et al. 2021; Ye et al. 2022). At a magnitude of up to 0.5 ns, x–p bias for these signals are no longer negligible, though, and should clearly be considered when processing BeiDou-3 data from heterogeneous receiver networks.

Summary and conclusions

Data + pilot biases as well as biases between observations from combined data + pilot tracking and pilot-only tracking have been measured for a comprehensive set of modern GNSS signals. Based on these measurements, it is shown that combined-minus-pilot-only biases for common receivers can be predicted from measured data + pilot biases and known power ratios with good confidence for most signals using a basic "multipath" model. For the dominating case of equal power sharing of the data and pilot components, they amount to 50% of the d–p biases. For the BDS-3 B1C and QZSS L1C signals with their 1:3 power sharing, a 37% bias ratio is predicted by the simple model, but smaller values may apply depending on the actual combining method and/or on the weighting of both components in a specific receiver architecture.

The measurements confirm the common expectation that data + pilot biases of time-multiplexed signals, i.e., GPS and QZSS L2C, and interlaced signals, such as GPS L1C are fully negligible. With representative magnitudes of 0.05 ns or less, the biases for these signals do not merit a distinction of data, pilot, and combined tracking modes in GNSS data processing. For Galileo, satellite-specific data + pilot biases in the E1 O/S, E5a, and E5b signals are confined to typically 0.1–0.3 ns, which limits associated inconsistencies in the clock offset determination to the 5 cm level when neglecting those contributions in the processing of observations from the combined tracking mode. With representative magnitudes of 1–2 ns, the data-minus-pilot and combined-minus-pilot-tracking biases are no longer negligible, though, for GPS L5, QZSS L1C, and BeiDou-3 B1C/B2a signals. Here, use of pre-determined x–p biases in the observation model enables a unified processing of measurements from receiver groups with x- and p-tracking in orbit determination and time synchronization as well as precise point positioning.

Declarations

References

Betz J (2016) Engineering satellite-based navigation and timing: global navigation satellite systems, signals, and receivers. Wiley, New York. https://doi.org/10.1002/9781119141167

Byun SH, Hajj GA, Young LE (2002) Development and application of a GPS signal multipath simulator. Radio Sci 37(6):1098. https://doi.org/10.1029/2001RS002549

Cabinet Office (2022a) MIRAI Multi-GNSS Integrated Real-time and Archived Information system, Government of Japan. https://go.gnss.go.jp/mirai/

Cabinet Office (2022b) Quasi-Zenith Satellite System Interface Specification Satellite Positioning, Navigation and Timing Service, IS-QZSS-PNT-005, 24 Oct 2022b. URL https://qzss.go.jp/en/technical/download/pdf/ps-is-qzss/is-qzss-pnt-005.pdf

CSNO (2017). BeiDou navigation satellite system signal in space interface control document: open service signal B1C (Version 1.0). China Satellite Navigation Office. URL http://www.beidou.gov.cn/xt/gfxz/201712/P020171226741342013031.pdf

Gunawardena S, Carroll M, Raquet J, van Graas F. (2015) High-fidelity signal deformation analysis of live sky Galileo E1 signals using a chip shape software GNSS receiver, In: Proceedings of the ION GNSS+ 2015, Tampa, FL, September 14–18, pp 3325–3334

Guo Y, Zou D, Wang X, Rao Y, Shang P, Chu Z, Lu X (2022) Method for estimating the optimal coefficient of L1C/B1C signal correlator joint receiving. Remote Sens 14(6):1401. https://doi.org/10.3390/rs14061401

Hauschild A, Montenbruck O (2016) The effect of correlator and front-end design on GNSS pseudorange biases for geodetic receivers. Navig J ION 63(4):441–451. https://doi.org/10.1002/navi.165

Hegarty CJ (1999) Evaluation of the Proposed Signal Structure for the New Civil GPS Signal at 1176.45 MHz. Working Note WN99W0000034, MITRE Corporation, McLean, VA. URL https://www.mitrecaasd.org/library/documents/gps_l5_signal.pdf

Javad (2022) GNSS receiver external interface specification (GREIS) reflecting firmware version 4.2.01, issued June 25, 2022, Javad GNSS

Johnston G, Riddell A, Hausler G (2017) The International GNSS Service. In: Teunissen PG, Montenbruck O (eds) Springer handbook of global navigation satellite systems. Springer, Berlin, pp 967–982. https://doi.org/10.1007/978-3-319-42928-1_33

Kogure S, Ganeshan AS, Montenbruck O (2017) Regional systems. In: Teunissen PG, Montenbruck O (eds) Springer handbook of global navigation satellite systems. Springer, Berlin, pp 305–337. https://doi.org/10.1007/978-3-319-42928-1_17

Li X, Li X, Liu G, Xie W, Guo F, Yuan Y, Zhang K, Feng G (2020) The phase and code biases of Galileo and BDS-3 BOC signals: effect on ambiguity resolution and precise positioning. J Geodesy 94(1):9. https://doi.org/10.1007/s00190-019-01336-9

Lu M, Li W, Yao Z, Cui X (2019) Overview of BDS III new signals. Navig J ION 66(1):19–35. https://doi.org/10.1002/navi.296

Marquis W, Shaw M (2011) Design of the GPS III space vehicle. In: Proceedings of the ION GNSS 2011. Institute of Navigation, Portland, OR, September 19–23, pp 3067–3075

Montenbruck O, Steigenberger P (2021) GNSS orbit determination and time synchronization. In: Morton J, van Diggelen F, Spilker JJ Jr, Parkinson B (eds) Position, navigation, and timing technologies in the 21st century: integrated satellite navigation, sensor systems, and civil applications. Wiley, New York. https://doi.org/10.1002/9781119458449.ch11

Montenbruck O, Hauschild A, Steigenberger P (2014) Differential code bias estimation using multi-GNSS observations and global ionosphere maps. Navig J ION 61(3):191–201. https://doi.org/10.1002/navi.64

Montenbruck O, Steigenberger P, Wang N, Hauschild A (2022) Characterization and performance assessment of BeiDou-2 and BeiDou-3 satellite group delays. Navig J ION 69(3). https://doi.org/10.33012/navi.526

Montenbruck O, Steigenberger P (2022) BRD400DLR: DLR's merged multi-GNSS broadcast ephemeris product in RINEX 4.00 format [DLR/GSOC]. https://doi.org/10.57677/BRD400DLR

Montenbruck O, Steigenberger P, Hauschild A (2020) Comparing the 'Big 4' – a user's view on GNSS performance, In: Proceedings of the IEEE/ION Position, Location and Navigation Symposium (PLANS), pp 407–418. https://doi.org/10.1109/PLANS46316.2020.9110208

Romero I (ed) (2021) RINEX the receiver independent exchange format version 4.00, 1 Dec 2021. https://files.igs.org/pub/data/format/rinex_4.00.pdf

RTCM (2021) 10403.3, Differential GNSS (Global Navigation Satellite Systems) Services – Version 3 + Amendment 2, 20 May 2021, Radio Technical Commission for Maritime Services, Arlington

Schaer S (2018) SINEX BIAS–Solution (Software/technique) Independent EXchange Format for GNSS Biases, Version 1.00, October 3, 2018. https://files.igs.org/pub/data/format/sinex_bias_100.pdf

Sleewaegen JM, Clemente F (2018) Quantifying the pilot-data bias on all current GNSS signals and satellites, IGS Workshop 2018, Wuhan

Spilker Jr JJ, Orr RS (1998) Code multiplexing via majority logic for GPS modernization. In: Proceedings of the ION GPS 1998, Institute of Navigation, Nashville, TN, September 15–18, pp 265–273

Thoelert S, Steigenberger P, Montenbruck O, Meurer M (2019) Signal analysis of the first GPS III spacecraft. GPS Solut 23:92. https://doi.org/10.1007/s10291-019-0882-7

USCG (2022) GPS Technical References – GPS III Satellites; United States Coast Guard Navigation Center. URL https://www.navcen.uscg.gov/gps-technical-references

Villiger A, Schaer S, Dach R, Prange L, Sušnik A, Jäggi A (2019) Determination of GNSS pseudo-absolute code biases and their long-term combination. J Geodesy 93(9):1487–1500. https://doi.org/10.1007/s00190-019-01262-w

Wang N, Yuan Y, Li Z, Montenbruck O, Tan B (2016) Determination of differential code biases with multi-GNSS observations. J Geodesy 90(3):209–228. https://doi.org/10.1007/s00190-015-0867-4

Wang E, Yang T, Wang Z, Zhang Y, Guo J, Shu W, Qu P (2021) Performance evaluation of precise point positioning for BeiDou-3 B1c/B2a signals in the global range. Sensors 21(17):5780. https://doi.org/10.3390/s21175780

Ye F, Yuan Y, Yang Z (2022) Validation and evaluation on B1IB3I-based and B1CB2a-based BDS-3 precise orbits from iGMAS. Adv Space Res 70(8):2167–2177. https://doi.org/10.1016/j.asr.2022.07.002

Young L, Meehan T (1988) GPS multipath effect on code-using receiver. AGU Spring Meeting, May 1988, Baltimore, MD

O. Montenbruck is head of the GNSS Technology and Navigation Group at DLR's German Space Operations Center (GSOC). His research activities include spaceborne GNSS receiver technology, autonomous navigation systems, spacecraft formation flying and precise orbit determination, new constellations, and multi-GNSS processing. Oliver Montenbruck presently chairs the Multi-GNSS Working Group of the International GNSS Service and coordinates the performance of the MGEX Multi-GNSS Pilot Project. He is a fellow of the Institute of Navigation (ION) and received the ION Johannes Kepler Award in 2018.

P. Steigenberger received his master's and a PhD degree in Geodesy from Technische Universität München (TUM) in 2002 and 2009, respectively. Currently, he is a senior researcher at DLR's German Space Operations Center (GSOC). His research interests focus on GNSS data analysis, particularly the precise orbit and clock determination of GNSS satellites and the evolving navigation systems of Galileo, BeiDou, and QZSS.

J. M. Sleewaegen is Lead Architect at Septentrio, Belgium, where he is responsible for GNSS signal processing, system design, and technology development since the company's inception in 1999. He received his MSc and PhD in electrical engineering from the Free University of Brussels. He received the ION Burka Award in 1999.